

Magnetic field of the K800 cyclotron

D. Johnson, T. Kuo, F. Marti, J. A. Nolen Jr., B. Sherrill, A. Zeller

Cyclotron Laboratory, NSCL, MSU, East Lansing, Mich

and

L. H. Harwood

CEBAF, Newport News, Virginia

Abstract. We present the results of the magnetic field mapping of the K800 superconducting cyclotron. The measured imperfections and their possible origins are discussed.

Introduction

The K800 is a 3 sector, 5 T heavy ion compact cyclotron with an extraction radius of 1.0 m. Like its predecessor the K500 (extraction radius of 0.66 m) it is injected vertically on the axis with an ion beam produced by one of two ECR ion sources, shared by the two cyclotrons. We are at the time of this conference commissioning this new cyclotron; tests with internal beam are in progress and the extraction hardware is nearing completion.

A new cycle of magnetic field measurements of the K800 cyclotron was performed in the last few months of 1987. This set of measurements was supposed to be the final one from which the data base for the trim coil fitting code would be created. The results of the previous mapping cycles have been described elsewhere [1].

The hardware utilized in the measurement has been described in previous reports [2], and only minor mechanical changes were performed to accommodate a new RF support structure. Basically the system consists of a search coil that is moved radially through the center of the machine towards the outside. The voltage generated by the changing flux is converted to pulses by a voltage to frequency converter. The number of pulses is then proportional to the magnetic field change between the center of the cyclotron (where it is determined by an NMR) and the observation point. The arm where the coil moves is then rotated to a new angular setting and the measurement repeated. The radial measurements are taken every 0.1 inches (2.54 mm) and typically every degree azimuthally, and each 360 degrees map is done in about one hour. The accuracy of the measurement has been determined to be 2 gauss out of 5 T.

Main Grid

A set of 16 maps were measured in a grid of the I_α, I_β plane, where I_α and I_β are the currents in the two sections of the superconducting coil. The grid covers the operating region of the cyclotron. Figure 1 shows the measured points, represented by solid squares. The grid spacing is approximately twice the original planned spacing. We decided to accelerate the mapping process in this way and postpone the decision on whether to perform the finer grid measurements until the internal beam tests had been completed, and the extraction elements installed.

Because some of the iron pieces in the return yoke had been machined and the magnet reassembled, it was necessary to center the cryostat and coil with respect to the pole tips. The first harmonic in the extraction region was used to position the cryostat.

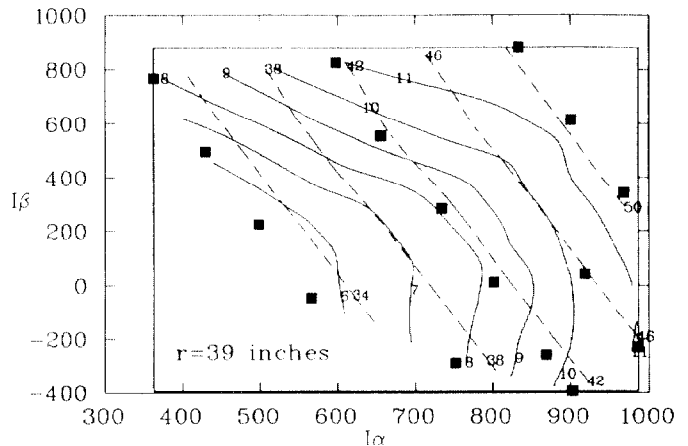


Fig. 1.- The median plane magnetic field was measured at 16 points (filled squares) with currents I_α and I_β in the main superconducting coils. The solid contour lines indicate points with equal first harmonic amplitude at $r=39$ inches, between 6 and 11 gauss. The dashed contour lines give the values for the average B field at $r=39$ between 34 and 50 kG.

The final position of the coil was determined by the forces on the radial links and the effect on the first harmonic.

Two of our extreme running conditions in the operating diagram are the so called $+/+$ mode ($I_\alpha=833$, $I_\beta=884$ A) and the $+/-$ mode ($I_\alpha=903$, $I_\beta=-394$ A). A polar plot of the three sector difference for those two maps is shown in Fig. 2. At each point we subtracted the average of the magnetic field at that location and the corresponding points 120 degrees apart. Ideally the cyclotron should have perfect 3-fold symmetry, and the three fold difference should be zero.

A contour map of the first harmonic error at $r=39$ inches is shown in Fig. 1. We have superimposed on the same picture the contour lines for the average magnetic field at $r=39$ (dashed lines).

At present we have been unable to identify unequivocally the sources of the field error. There are several possible sources. The yoke penetrations have been compensated assuming that what counts is to have the iron masses azimuthally compensated at each radius and z value. This approach neglects the different magnetization in the yoke due to the different hole sizes and presence of neighbouring holes.

Another effect which may be contributing to the magnet imperfections is the change in gap between the upper and lower pole caps with increasing magnetic field. The large forces on the caps attract them to each other so strongly that the pole tip gap is reduced by 1.5 mm when the coils are fully excited ($+/+$ case). The load is partially transferred to the

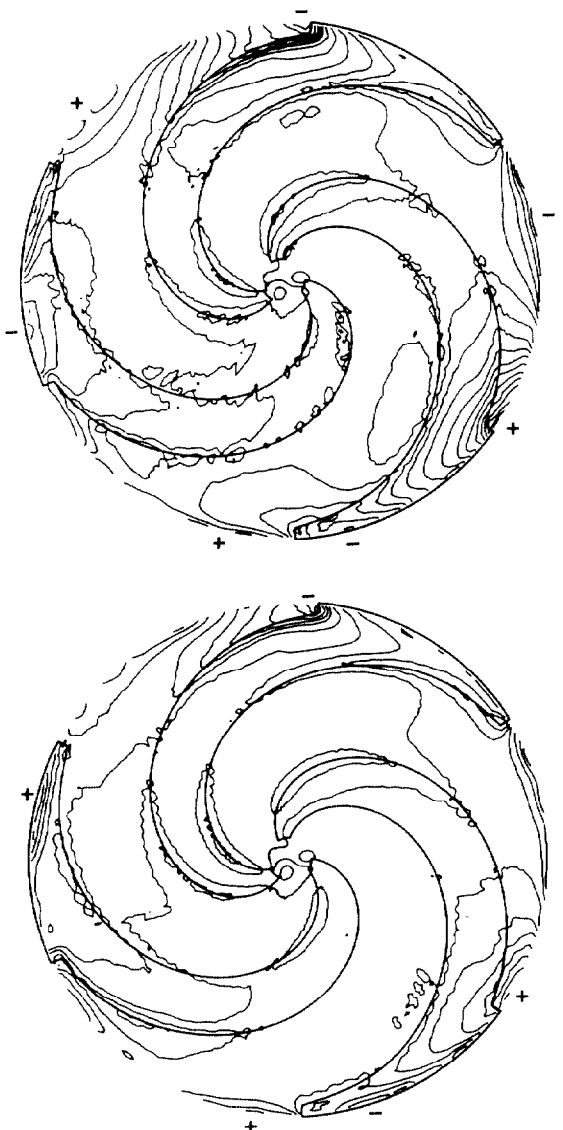


Fig. 2.- Contour lines (every 5 gauss) indicating the errors in the magnetic field with respect to the three sector average. Top $+/-$ (833/884 A) and bottom $+/-$ (903/394 A). These plots show the error fields and their location with respect to the pole tips. An absolute excess field of 1 gauss at a given location will appear as an excess of $2/3$ at that point and as a defect of $1/3$ at the other two points 120 degrees away.

cryostat and will produce an azimuthally differential decrease of the cryostat inner wall (just beyond the pole tip edges in Fig. 2). Small changes in the azimuthal position of the pole tips could also contribute to the field error. The comparison of the contour lines for the first harmonic amplitude in Fig. 1 with the contour lines of vertical forces on the coil shown in reference [3] indicates a striking similarity. This seems to indicate that the main cause of the imperfections is associated with displacement of steel pieces when the stresses on the magnet increase.

An interesting feature of the data is the variation of the phase and amplitude of the third harmonic (main contribution to the flutter) with coil excitation. Figure 3 shows a contour map of the differences in amplitude at a radius of 33 inches. The upper part shows the amplitude variation relative

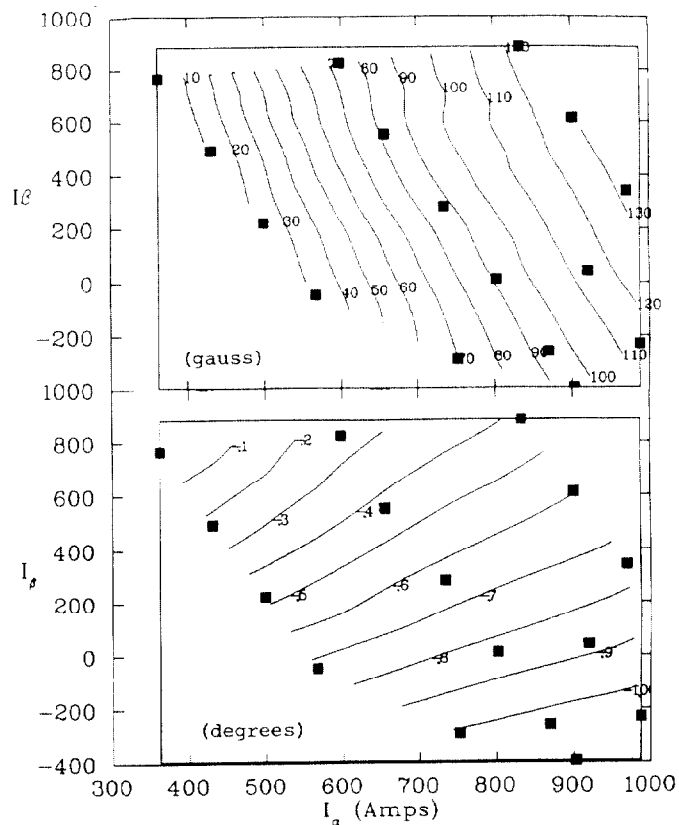


Fig. 3.- Systematics of the third harmonic amplitude (top) and phase (bottom) in the I_a, I_3 plane for $r=33$ inches. The values are with respect the upper left corner measured point.

to the upper left measurement, and the lower part of the figure shows the phase variation with respect to the same point. It is a smooth and continuous mapping of the excitation plane. We have used a simple model to try to demonstrate that this behavior is a 3-dimensional effect. Our magnetic fields are calculated with the computer code POISSON using an azimuthally symmetric magnet with stacking factors that simulate the reduced amount of iron in regions like the pole tips and RF stem holes. The contribution of these reduced iron rings are then subtracted from the average field and uniform fully saturated pieces of iron with the correct shape are replaced in the magnet and their field calculated exactly. This approach does not allow for any r or θ component to the magnetization. In our simple model the value of the magnetization is still constant, but the direction in the $r-z$ plane is obtained from the POISSON calculation. No θ component is included. The change in phase is approximated by the model, but the amplitude changes are not. The θ component is probably quite important, and it is necessary to use a fully 3-d model to obtain a better understanding of this detailed behavior. The large number of points required to model in 3-dimensions a complex magnet make it unrealistic to use only 3-D codes at the present time.

Extraction calculations

The effect of the field imperfections on the orbit behavior in the extraction region has been studied for a few beams. So far it has been possible

to compensate the imperfections with an extraction bump provided by trim coil 21. The beam can be kept centered up to the $\nu_r=1$ resonance without a major perturbation of the phase space. The few internal beams that we have run so far indicated an excellent agreement (1 kHz or less error) with the calculated frequency.

Trim coil fields

The magnetic fields of the 21 (per hill) trim coils have been measured at four different I_α , I_β excitations. The four points are on the boundaries of the operating diagram and intermediate excitations are obtained by linear interpolation in these four. Figure 4 shows the average fields of 4 trim coils for one of these measurements (solid line). The theoretical (air core) calculation is shown as the dashed lines. In general, the trim coil fields are stronger than the air core calculation by peak percentage deviations ranging from 32 % at the least saturated field to 17 % for the full $+/+$ field.

Axial fields

The magnetic field along the vertical injection line on the cyclotron axis has been measured at four different excitations. A search coil with the same electronics used in the median plane measurements was employed, but without computer control. These fields are used in the axial injection calculations. Figure 5 shows the comparison with a Poisson calculation. As we see the data and calculation are very close, except for details at the entrance of the yoke $z = 60$ inches due to the support structure not included in the calculation.

Conclusions

After an initial period of debugging the hardware associated with the K800 mapper, the system performed an excellent job in measuring the magnetic field of the cyclotron up to the 6 T level. The reproducibility and smoothness of the measurements gives us confidence on the results. The symmetry errors in the extraction region, although smaller than the K500 cyclotron are larger than we expected. Several factors are probably contributing to the imperfections. Orbit calculations have shown these errors to be tolerable. The Poisson calculations are accurate enough to determine the field on the axis, used in axial injection studies. A fully 3-d magnetic code is necessary to understand the details of the magnetic field, although POISSON plus current sheet model proved adequate for producing the cyclotron magnet with no shimming required.

References

- [1] Harwood, L. H., J. A. Nolen and A. F. Zeller, Proc. 11th Int. Conf. on Cyclotrons, (Ionics, Tokyo) 1987, 315.
- [2] Harwood, L. H., J. A. Nolen, Proc. 10th Int. Conf. on Cyclotrons, (IEEE, East Lansing) 1984, 101.
- [3] Milton, B.F. and L.H. Harwood, NSCL Annual Report 1983-1984, p.224.

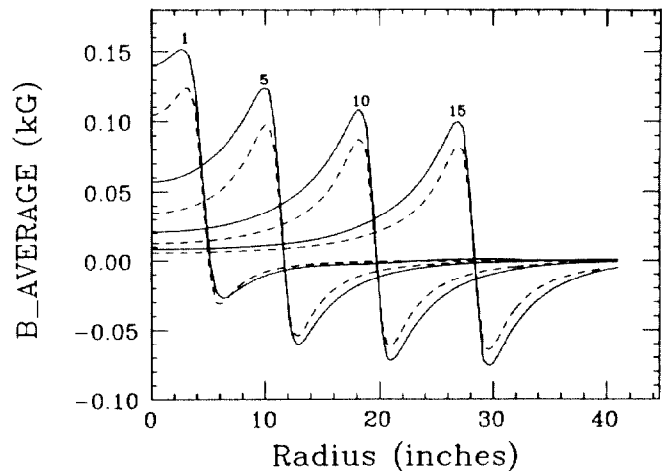


Fig. 4.- Comparison of measured (solid line) and calculated, air core coil, (dashed line) average fields. This group ($I_\alpha = 633.9$, $I_\beta = -317.5$) is one of the four measured sets.

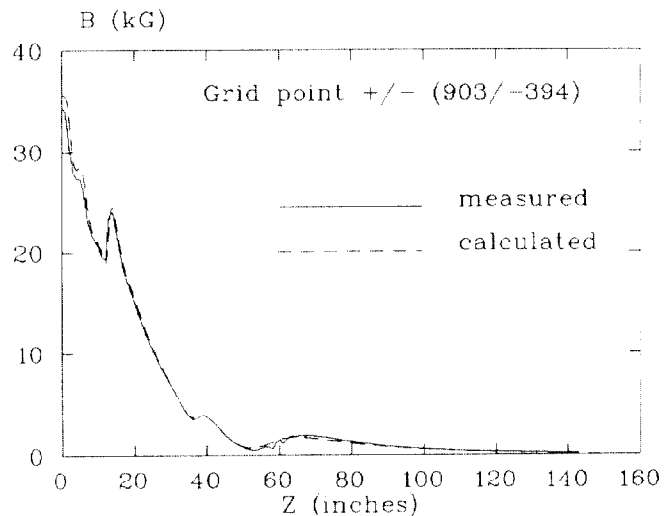


Fig. 5.- Axial fields as a function of distance to the median plane. Comparison of measurements with the POISSON calculation of the axial field.